# Electron-induced excitation of vibrations of Ce atoms inside a C<sub>80</sub> cage

A. Stróżecka, <sup>1,2,\*</sup> K. Muthukumar, <sup>3,†</sup> J. A. Larsson, <sup>3</sup> A. Dybek, <sup>4</sup> T. J. S. Dennis, <sup>4</sup> J. Mysliveček, <sup>5</sup> and B. Voigtländer <sup>1</sup> Peter Grünberg Institut (PGI-3), and JARA, Fundamentals of Future Information Technology, Forschungszentrum Jülich, D-52425 Jülich, Germany

<sup>2</sup>Institut für Experimentalphysik, Freie Universität Berlin, Arnimallee 14, D-14195 Berlin, Germany 
<sup>3</sup>Tyndall National Institute, University College Cork, Lee Maltings, Prospect Row, Cork, Ireland 
<sup>4</sup>Department of Physics, Queen Mary, University of London, Mile End Road, London E1 4NS, United Kingdom 
<sup>5</sup>Charles University, Faculty of Mathematics and Physics, V Holešovičkách 2, Praha 8, Czech Republic 
(Received 15 June 2010; revised manuscript received 2 February 2011; published 14 April 2011)

Inelastic electron tunneling spectroscopy of  $Ce_2@C_{80}$  dimetallofullerenes reveals a low-energy inelastic excitation that is interpreted using *ab initio* calculations and associated with the movements of encapsulated Ce atoms inside the  $C_{80}$  cage. The electron-vibration interaction in  $Ce_2@C_{80}$  is unusually high, inducing a pronounced zero-bias anomaly in differential conductance of  $Ce_2@C_{80}$ . Our observations show that the atoms encapsulated in fullerene cages can actively participate in determining the properties of molecular junctions.

DOI: 10.1103/PhysRevB.83.165414 PACS number(s): 82.37.Gk, 71.20.Tx, 73.63.Rt

#### I. INTRODUCTION

Electron-vibration interactions are known to influence the properties of single-molecule electronic junctions<sup>1</sup> like the current-to-voltage characteristics<sup>2</sup> or the current limit.<sup>3</sup> Experimentally, electron-vibration interactions are often studied in model single-molecule junctions realized in scanning tunneling microscope (STM) where one electrode (the STM tip) is connected to the molecule/counter electrode setup via a tunneling gap. In such junctions, the opening of inelastic tunneling channels allows the detection of single-molecule vibrations through inelastic electron tunneling spectroscopy (IETS).<sup>4</sup>

Fullerenes represent prototypical molecules for single-molecule junction studies. For the single  $C_{60}$  the stability, the conductance, and the electron-vibration fingerprint in different junction geometries have been thoroughly studied. Functionality of empty fullerene cages is expected to become significantly more complex on endohedral doping, when atoms or molecules are enclosed in the carbon cages of fullerenes. A study of  $Ce_2@C_{80}$  showed that the doping directly influences the conductance of the corresponding molecular junction. Generally, the atoms and molecules inside the fullerene cages are very well screened from the external physical and chemical influences. Influences. As a consequence, no vibration excitations of the encapsulated atoms were found in previous single-molecule electronic junction studies on endofullerenes.

Here we present evidence for the electron-vibration excitation of Ce atoms encaged in a  $C_{80}$  fullerene ( $Ce_2@C_{80}$ ). Inelastic electron tunneling spectroscopy together with *ab initio* calculations indicate that the lowest-energy excitations in the IETS spectrum of  $Ce_2@C_{80}$  represent the vibrations of Ce atoms inside the  $C_{80}$  cage. The endohedral doping of  $Ce_2@C_{80}$  also contributes to enhancing the overall cross section of the electron-vibration excitation in the molecular junction. We observe a massive increase of the tunneling conductance by a factor of 2 in the energy range of the excited vibrations, leading to a pronounced zero-bias conductance anomaly and a distinct nonlinearity in the current-to-voltage characteristics of the single-molecule junction. Our experiments

show that the atoms inside fullerene cages can significantly influence the characteristics of the corresponding molecular junctions.

## II. EXPERIMENTAL

The experiments were performed with a commercial ultrahigh vacuum STM operated at  $T=6~\rm K.~Ce_2@C_{80}$  metallofullerenes were isolated from soot by high-performance liquid chromatorgaphy (HPLC) as described in Ref. 14. Cu(111) substrates were cleaned by repeated cycles of Ne<sup>+</sup> sputtering and vacuum annealing. Ce<sub>2</sub>@C<sub>80</sub> molecules were evaporated from a Knudsen cell on a clean Cu(111) surface held at room temperature. Experiments with Ce<sub>2</sub>@C<sub>80</sub> on Cu(111) were complemented by reference measurements with Ce@C<sub>82</sub> (Refs. 14 and 15) and C<sub>60</sub> (Ref. 10) on Cu(111) and with Ce<sub>2</sub>@C<sub>80</sub> on Au(111).

STM measurements were performed with electrochemically etched W tips treated by interactions with the Cu(111) substrate until delivering tunneling spectra corresponding to clean Cu(111). Measurements of the current-to-voltage (I/V) characteristic of the tunneling junctions and their first (dI/dV) and second  $(d^2I/dV^2)$  derivatives were performed at a constant tip-sample separation given by the set current  $I_0 = 0.5$  nA and the set sample bias  $V_0 = 150$  mV before switching off the feedback of the STM. dI/dV and  $d^2I/dV^2$  were measured by two lock-in amplifiers using bias voltage modulation with the frequency of  $\approx 360$  Hz and the rms amplitude 6 mV. We realized and analyzed about 80 single-molecule junctions with Ce<sub>2</sub>@C<sub>80</sub>.

#### III. IETS OF CE2@C80

The schematic of the adsorption of  $Ce_2@C_{80}$  on Cu(111) is shown in Fig. 1(a). The Ce atoms are enclosed in the  $I_h$  isomer of the  $C_{80}$  cage. <sup>14</sup> The adsorption geometry with the sixmembered ring parallel to the surface and the positions of the Ce atoms in the adsorbed molecule have been established by previous calculations. <sup>10,16</sup> On deposition at room temperature (RT),  $Ce_2@C_{80}$  nucleate in small islands on Cu(111) planes. A detail of such island is shown in the STM image in Fig. 1(b).

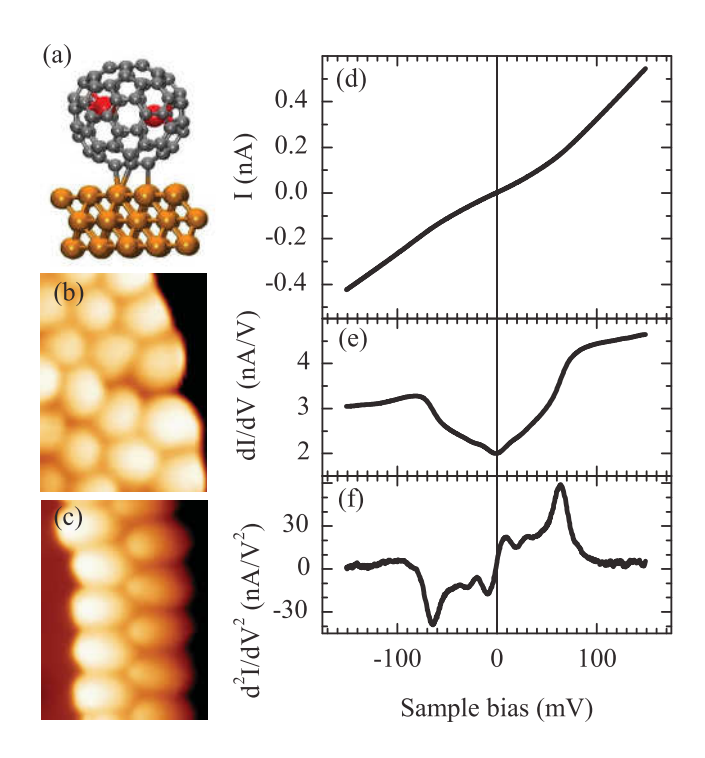


FIG. 1. (Color online) Ce<sub>2</sub>@C<sub>80</sub> molecules adsorbed on the Cu(111) surface. (a) Schematic, (b) STM image after deposition at RT, and (c) annealed to 250 °C. Image width in (b) and (c) is 4 nm. [(d)–(f)] A pronounced fingerprint of the electron-vibration excitations of Ce<sub>2</sub>@C<sub>80</sub> in the I/V characteristic of the tunneling junction and its derivatives.

The adsorption position of  $Ce_2@C_{80}$  can be modified by annealing to 250 °C, after which the molecules decorate the step edges of Cu(111) as shown in the STM image in Fig. 1(c). Regardless of the sample bias applied,  $Ce_2@C_{80}$  reveal no intramolecular structure and always appear in the images as featureless protrusions, in contrast to  $C_{60}$  on Cu(111).  $^{10,17}$ 

A typical IETS of the  $Ce_2@C_{80}$  is shown in Figs. 1(d)-1(f). The I/V curve [Fig. 1(d)] shows a visible nonlinearity—a decrease of the differential conductance in the proximity of zero bias. In dI/dV, a pronounced zero-bias conductance anomaly becomes apparent [Fig. 1(e)]. Finally, the  $d^2I/dV^2$  [Fig. 1(f)] shows pronounced symmetric peaks and dips characteristic of inelastic electron tunneling. <sup>18</sup> Each peak corresponds to opening of one of several inelastic electron tunneling channels with increasing bias voltage. We attribute the inelastic losses to the excitation of molecular vibrations of  $Ce_2@C_{80}$ . The distinct influence of the electron-vibration excitation on the I/V curve of the molecular junction indicates an unusually high cross section of this process.

In the voltage region of a few millielectron volts,  $d^2I/dV^2$  curves measured on molecules often exhibit features lacking the necessary symmetry and/or show too much correlation to the  $d^2I/dV^2$  curve of the bare substrate to qualify for electron-vibration excitations. We revisit the lowest-energy  $d^2I/dV^2$  peaks of the Ce<sub>2</sub>@C<sub>80</sub> molecule on a detailed view in Fig. 2. We observe that these peaks do have the symmetry required for the qualification as inelastic excitations. A comparison to the

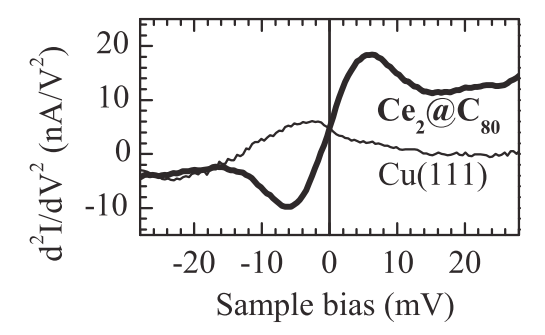


FIG. 2. Detail of  $d^2I/dV^2$  curve measured over a  $\text{Ce}_2@\text{C}_{80}$  molecule (thick line) compared to a bare Cu(111) substrate (thin line). The symmetry and the absence of substrate-related features classifies the  $d^2I/dV^2$  measured over the molecule as a fingerprint of a low-energy electron-vibration excitation.

 $d^2I/dV^2$  curve measured on the bare substrate also shows that the lowest-energy vibrations are a property of the Ce<sub>2</sub>@C<sub>80</sub> molecule and not an artifact from the STM tip and/or from the substrate.

The conductance anomaly as shown in Fig. 1(e) is observed for all investigated Ce2@C80 molecules. A selection of  $d^2I/dV^2$  curves illustrating the common features and the differences of the individual molecular junctions is shown in Fig. 3. In each  $d^2I/dV^2$  curve, we mark the positions of the peaks that have an antisymmetric counterpart and thus correspond to a vibration excitation. Common to all junctions are the excitations between 6 and 11 meV (Ref. 19) and between 60 and 65 meV. We label these excitations  $\nu_1$  and  $\nu_2$ , respectively. Apart from  $\nu_1$  and  $\nu_2$ , up to three excitations with intermediate or higher energies are present. The observation of  $v_1$  and  $v_2$  is robust: they are observed for  $Ce_2@C_{80}$  on Cu(111) deposited at RT [Figs. 3(a)-3(c)] as well as annealed to 250 °C [Figs. 3(d)-3(f)], and in a reference experiment with Ce2@C80 deposited at RT on Au(111) [Fig. 3(g)]. Especially, the  $v_1$  represents an excitation characteristic of the Ce<sub>2</sub>@C<sub>80</sub> molecule. This has been confirmed by further reference experiments: the  $v_1$  is absent in C<sub>60</sub> on Cu(111) and single-doped metallofullerene Ce@C<sub>82</sub> molecules on Cu(111).  $\nu_1$  and  $\nu_2$  exhibit small, and the other observed vibrations somewhat larger variations of energy and amplitude which we attribute to the availability of different adsorption sites, <sup>10</sup> varying numbers of neighboring Ce<sub>2</sub>@C<sub>80</sub> molecules, and variations caused by a strong localization of the IETS signal over a single fullerene cage. 13 Calculating the normalized change in the differential conductance, defined as  $\Delta \sigma / \sigma$ , where  $\sigma = dI/dV$ , we obtain electron-vibration cross sections 15–20% for  $v_1$ , 30–40% for  $v_2$ , and 5–15% for other observed excitations. The values for  $v_1$  and  $v_2$  exceed the values commonly observed in the IETS experiments on fullerenes<sup>7,13</sup> and other molecules<sup>20</sup> that stay below 15%.

The unambiguous (cf. Fig. 2) and intensive low-energy excitation has not been observed in previous STM-IETS studies on empty fullerenes ( $C_{60}$  in Refs. 7 and 17) and endohedrally doped fullerenes ( $Gd@C_{82}$  in Ref. 13). We will discuss the nature of this highly intriguing IETS feature based on *ab initio* calculations of electron-vibration coupling in  $Ce_2@C_{80}$ . In the discussion we rule out the possibility

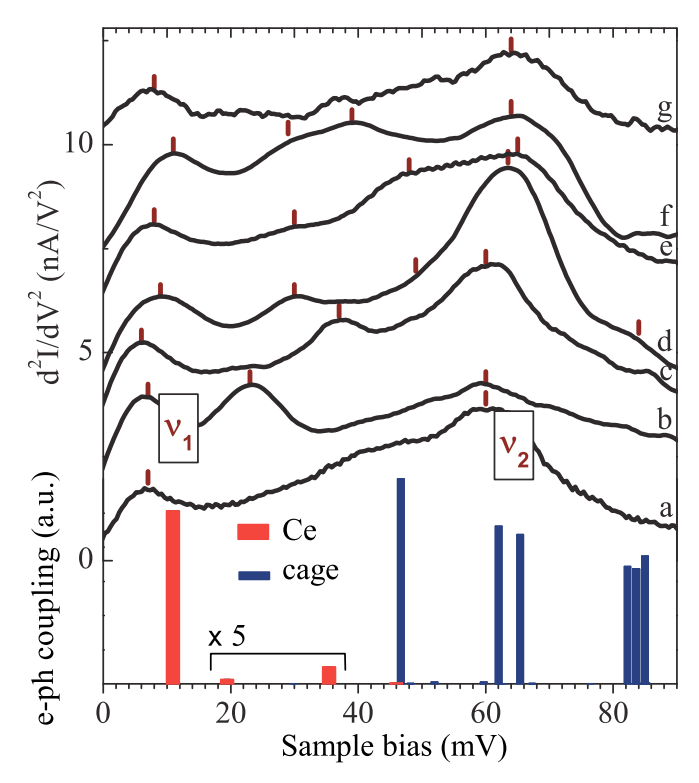


FIG. 3. (Color online)  $d^2I/dV^2$  vibration spectra of  $Ce_2@C_{80}$  molecules [(a)–(c)] on Cu(111), deposited at RT, [(d)–(f)] on Cu(111), annealed to 250 °C, (g) on Au(111), deposited at RT. Peaks corresponding to vibrations are marked by vertical bars. Vibrations common to all observed molecules between 6 and 11 meV and between 60 and 65 meV are labeled  $\nu_1$  and  $\nu_2$ , respectively. The bar graph shows electron-vibration coupling calculated for the vibration modes of a free  $Ce_2@C_{80}$  molecule. Vibrations that involve movements of Ce atoms are shown in red (broad bars).

that the low-energy excitation is due to molecule-substrate movements (bouncing). Observation of bouncing in fullerenes has been limited to non–STM IETS experimental setups so far ( $C_{60}$  in Ref. 2). Rather, we propose that the  $\nu_1$  is due to movements of Ce with respect to the  $C_{80}$  cage. Our proposal is based on the observation that the Ce-cage vibration modes occupy the lowest energies in the Raman spectra of endohedral metalofullerenes.  $^{21,22}$ 

## IV. CALCULATION OF CE VIBRATIONS

In the following, we are discussing the observed vibrations based on the results of ab-initio calculations. We evaluate the cross section for exciting an inelastic electron-vibration tunneling channel as

$$\Delta \rho_i \approx \left| \frac{dE_{E_F}}{dQ_i} \frac{\hbar}{\sqrt{2m_i^* \Omega_i}} \right|^2,$$
 (1)

where  $E_{E_F}$  is the energy of a molecular orbital inelastically coupling at the Fermi level, and  $Q_i$ ,  $m_i^*$ , and  $\Omega_i$  are the normal coordinate, the reduced mass, and the frequency of the  $i^{\text{th}}$  molecular vibration, respectively. Equation (1) represents a useful approximation for discussing the IETS of endofullerenes.<sup>13</sup> In order to make the *ab initio* analysis

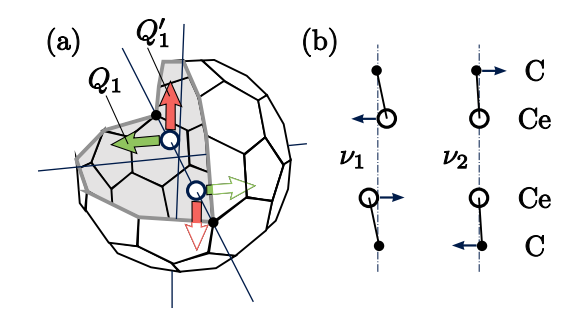


FIG. 4. (Color online) (a) Schematic of the Ce motions inside the  $C_{80}$  cage corresponding to the  $\nu_1$  electron-vibration excitation. The  $\nu_1$  has  $e_g$  symmetry, is twofold degenerate  $(Q_1, Q_1')$ , and involves motions of Ce atoms parallel to the C cage. (b) Displacements of atoms on the C–Ce–Ce axis for  $\nu_1$  at 11 meV and  $\nu_2$  at 65 meV. The positions of the atoms correspond to the calculated turning point of the vibration; the arrows indicate the direction of the atom motion.

feasible, we calculated the electron-vibration cross sections of a free Ce<sub>2</sub>@C<sub>80</sub>. We used unrestricted density functional theory (DFT) as implemented in TURBOMOLE 5.10.<sup>23</sup> Details of the calculations are given in a previous work where the ground state and the infrared (IR) vibration spectrum of Ce<sub>2</sub>@C<sub>80</sub> have been determined.<sup>16</sup> The derivative of the highest occupied molecular orbital (HOMO) energy with respect to  $Q_i$  ( $dE_{E_F}/dQ_i$ ) was calculated numerically, displacing the atoms by 0.05 Å in directions given by  $Q_i$  and evaluating the corresponding change of the HOMO energy.<sup>24</sup>

The calculated energies of the vibration modes of  $Ce_2@C_{80}$  and the electron-vibration coupling with the HOMO of the molecule are plotted as a bar graph in Fig. 3. The calculations predict 58 vibration modes in the energy range up to 90 meV. Of these modes, only some are electron-vibration active, but of the active modes several have a significant contribution from Ce movements. We distinguish the vibration modes based on their effective mass  $m_i^*$ : the modes with  $m_i^* > 12.5$  (compared to 12.011 for pure carbon cage modes) are considered Ce active. In Fig. 3 these modes are shown in red.

### V. DISCUSSION

The calculations indicate that the experimentally observed vibration  $\nu_1$  can be identified with a theoretically predicted inelastic excitation with an energy of 11 meV. This excitation involves Ce motions inside the  $C_{80}$  cage (cf. Fig. 3). We show the schematic of the  $\nu_1$  vibration as obtained from the *ab initio* calculations in Fig. 4(a).  $\nu_1$  is twofold degenerate, has  $e_g$  symmetry, and involves the motions of Ce atoms perpendicular to the C–Ce–Ce–C axes (parallel to the  $C_{80}$  cage). The calculated Ce vibration modes at higher energies have a significantly lower electron-vibration activity. The mode at 19 meV has  $a_{1g}$  symmetry and represents Ce–Ce stretching. A mode with the same symmetry has been identified as the lowest-energy mode in  $La_2@C_{80}$ . The mode at 35 meV has  $a_{1g}$  symmetry as well and includes Ce–C

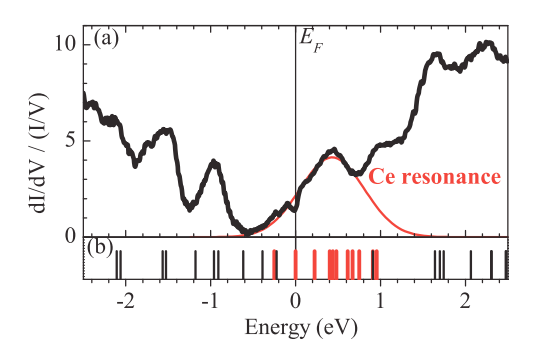


FIG. 5. (Color online) (a) Density of electron states of the  $Ce_2@C_{80}$  molecule measured by STS. The Ce resonance is crossing the Fermi level. The red curve is a fit to the experimental data. (b) Calculated electron states of a free  $Ce_2@C_{80}$  molecule. States with a >80% Ce contribution are marked red (broad bars). The Ce-dominated states have energies between (-0.2, 1.2) eV, and include both the HOMO and the LUMO of the molecule. The Ce-dominated states form a resonance near  $E_F$  also in an adsorbed molecule.  $^{10}$ 

stretching along the C–Ce–Ce–C axis (perpendicular to the  $C_{80}$  cage).

Calculated cage vibration modes appear at energies  $\geqslant$  27 meV. However, a significant electron-vibration cross section is calculated only for cage modes at energies  $\geqslant$ 47 meV. The electron-vibration excitations at 62 and 65 meV correspond to the experimental peak  $\nu_2$ . The assignment of the smaller experimental vibration peaks between  $\nu_1$  and  $\nu_2$ , and above  $\nu_2$ , to the calculated Ce and/or cage modes is less straightforward. Particularly, strong calculated modes at 47 and 85 meV are marginal in the experimental IETS, which may reflect differences between the free (calculation) and the adsorbed molecule (experiment).

The unusually high cross section for the electron-vibration excitation in Ce<sub>2</sub>@C<sub>80</sub> can be traced back to a coincidence of favorable conditions enhancing the IETS signal that is related to the unique electron structure of Ce<sub>2</sub>@C<sub>80</sub>. In Ref. 10 we have shown that orbitals of the encapsulated Ce atoms localize strongly both in space and in energy and that they separate both in space and energy from the cage orbitals. This situation is illustrated in Fig. 5 where we plot the density of states (DOS) of the adsorbed molecule as measured by STS [Fig. 5(a)] and the electron levels of a free molecule from the present calculation [Fig. 5(b)].<sup>26</sup> In the calculated data, we mark the electron levels of orbitals with >80% Ce contribution red. We observe that the Ce orbitals form a multiplet at and above the  $E_F$ , approximately between 0 and 1 eV. The cage orbitals, on the other hand, are observed exclusively outside this energy range. This allows us to identify and fit the Ce resonance in the experimental STS data [red line in the Fig. 5(a)].

Generally, the position of the molecular resonance participating in the inelastic tunneling with respect to  $E_F$  is a main factor determining the sign and the size of the inelastic conductivity change. Experiments on  $C_{60}$  show that the IETS cross section becomes maximized, when the molecular resonance is tailing  $E_F$ . This is the case for the Ce resonance in our experiment [Fig. 5(a)] and the first favorable condition

for the high IETS cross section in  $Ce_2@C_{80}$ . The strength of the electron-vibration interaction further increases with decreasing molecule-electrode coupling. 1.29 In recent conductivity measurements on single  $Ce_2@C_{80}$ , we have demonstrated that for the localized Ce orbitals the molecule-electrode coupling is significantly reduced, 10 which represents the second favorable condition for a large IETS cross section. Finally, the multiplet character of the Ce resonance in  $Ce_2@C_{80}$  may contribute to establishing of inelastic transmission channels for many different contact geometries and thus to weakening the restrictions to the availability of such channels that can be imposed by the symmetry of the electrodes in the single-molecule contact.  $^{1,30}$ 

The Ce vibration modes at 11 meV ( $v_1$ ) and 35 meV induce movements of Ce atoms in different directions with respect to the C<sub>80</sub> cage. Mutual Ce–C movements are observed also for the cage modes at higher energy. An example is displayed in Fig. 4(b) where the cage vibration at 65 meV  $(v_2)$  induces displacements of C atoms perpendicular to the C-Ce-Ce-C axis, complementary to the movements observed in the  $v_1$  mode. We can speculate that in the low-temperature STM IETS the highly effective electron-vibration excitation of  $v_1$  and higher-energy vibrations induces hopping of Ce atoms between the equivalent positions inside the C<sub>80</sub> cage. Such hopping of endohedral atoms inside the C<sub>80</sub> cage has been reported to appear spontaneously in La<sub>2</sub>@C<sub>80</sub> at room temperature<sup>31</sup> when the activation energy for hopping in the order of tens of millielectron volts (Ref. 25) is supplied by thermal fluctuations.

## VI. CONCLUSIONS

We are presenting inelastic electron tunneling spectroscopy of single Ce2@C80 molecules in scanning tunneling microscope together with ab initio analysis of electron-vibration coupling in Ce<sub>2</sub>@C<sub>80</sub>. We are observing a low-energy inelastic tunneling excitation in Ce2@C80 that can be interpreted as excitation of movements of encapsulated Ce atoms inside C<sub>80</sub> cage. The Ce-cage vibration and pure cage vibrations in Ce<sub>2</sub>@C<sub>80</sub> exhibit a very high electron-vibration coupling resulting in a pronounced zero-bias conductance anomaly in STM-IETS of Ce2@C80. We trace this unique behavior of Ce2@C80 back to its electron structure, where the orbitals localized on the Ce atoms are forming a strong band at energies between 0 and 1 eV above  $E_F$ , and mediate the electron-vibration interactions in Ce<sub>2</sub>@C<sub>80</sub>. Our observations show that encaged atoms can significantly influence the dynamics of fullerene-based molecular junctions.

#### **ACKNOWLEDGMENTS**

This work was supported by the FP6 Marie Curie Early Stage Training Network NANOCAGE (MEST-CT-2004-50-6854), Science Foundation Ireland, and the Ministry of Education of the Czech Republic (MSM 0021620834). We acknowledge the SFI/HEA Irish Centre for High-End Computing (ICHEC) for generous allotment of computer resources. We thank J. I. Pascual and K. J. Franke for many helpful discussions.

- \*anna.strozecka@physik.fu-berlin.de
- †Present address: Department of Chemical and Materials Engineering, University of Cincinnati, Cincinnati, 45220 OH, USA.
- <sup>1</sup>M. Galperin, M. A. Ratner, A. Nitzan, and A. Troisi, Science **319**, 1056 (2008).
- <sup>2</sup>H. Park, J. Park, A. K. L. Kim, E. H. Anderson, A. P. Alivisatos, and P. L. McEuen, Nature 407, 57 (2000); L. H. Yu and D. Natelson, Nano Lett. 4, 79 (2004).
- <sup>3</sup>M. Galperin, M. A. Ratner, and A. Nitzan, J. Phys. Condens. Matter **19**, 103201 (2007); G. Schulze, K. J. Franke, and J. I. Pascual, New J. Phys. **10**, 065005 (2008).
- <sup>4</sup>B. C. Stipe, M. A. Rezaei, and W. Ho, Science **280**, 1732 (1998).
   <sup>5</sup>C. Joachim, J. K. Gimzewski, R. R. Schlittler, and C. Chavy, Phys. Rev. Lett. **74**, 2102 (1995).
- <sup>6</sup>N. Neél, J. Kröger, L. Limot, T. Frederiksen, M. Brandbyge, and R. Berndt, Phys. Rev. Lett. **98**, 065502 (2007); N. Neél, J. Kröger, L. Limot, and R. Berndt, Nano Lett. **8**, 1291 (2008).
- <sup>7</sup>J. I. Pascual, J. Gómez-Herrero, D. Sánchez-Portal, and H. P. Rust, J. Chem. Phys. **117**, 9531 (2002).
- <sup>8</sup>K. J. Franke, G. Schulze, and J. I. Pascual, J. Phys. Chem. Lett. 1, 500 (2010).
- <sup>9</sup>H. Shinohara, Rep. Prog. Phys. **63**, 843 (2000).
- <sup>10</sup>A. Stróżecka, K. Muthukumar, A. Dybek, T. J. Dennis, J. A. Larsson, J. Mysliveček, and B. Voigtländer, Appl. Phys. Lett. 95, 133118 (2009).
- <sup>11</sup>P. Delaney and J. C. Greer, Appl. Phys. Lett. **84**, 431 (2004); K. Schulte, L. Wang, P. J. Moriarty, J. Purton, S. Patel, H. Shinohara, M. Kanai, and T. J. S. Dennis, Phys. Rev. B **71**, 115437 (2005).
- <sup>12</sup>W. Harneit, Phys. Rev. A **65**, 032322 (2002).
- <sup>13</sup>M. Grobis, K. H. Khoo, R. Yamachika, X. Lu, K. Nagaoka, S. G. Louie, M. F. Crommie, H. Kato, and H. Shinohara, Phys. Rev. Lett. 94, 136802 (2005).
- <sup>14</sup>M. Kanai, T. J. S. Dennis, and H. Shinohara, Am. Inst. Phys. Conf. Proc. **633**, 35 (2002).
- <sup>15</sup>L. Wang, K. Schulte, R. A. J. Woolley, M. Kanai, T. J. S. Dennis, J. Purton, S. Patel, S. Gorovikov, V. R. Dhanak, E. F. Smith, B. C. C. Cowie, and P. Moriarty, Surf. Sci. 564, 156 (2004).
- <sup>16</sup>K. Muthukumar and J. A. Larsson, J. Mater. Chem. 18, 3347 (2008).

- <sup>17</sup>J. A. Larsson, S. D. Elliott, J. C. Greer, J. Repp, G. Meyer, and R. Allenspach, Phys. Rev. B 77, 115434 (2008); A. Stróżecka, J. Mysliveček, and B. Voigtländer, Appl. Phys. A 87, 475 (2007).
- <sup>18</sup>W. Ho, J. Chem. Phys. **117**, 11033 (2002).
- <sup>19</sup>Technically, 6 mV is the lowest-energy peak that can be obtained from IETS measurement with 6-mV rms modulation. The actual energy of the corresponding inelastic excitation may eventually be lower.
- <sup>20</sup>B. C. Stipe, M. A. Rezaei, and W. Ho, Rev. Sci. Inst. **70**, 137 (1998).
- <sup>21</sup>R. Jaffiol, A. Débarre, C. Julien, D. Nutarelli, P. Tchénio, A. Taninaka, B. Cao, T. Okazaki, and H. Shinohara, Phys. Rev. B 68, 014105 (2003).
- <sup>22</sup>M. Krause, P. Kuran, U. Kirbach, and L. Dunsch, Carbon 37, 113 (1999).
- <sup>23</sup>R. Ahlrichs, M. Bär, M. Häser, H. Horn, and C. Kölmel, Chem. Phys. Lett. **162**, 165 (1989); O. Treutler and R. Ahlrichs, J. Chem. Phys. **102**, 346 (1995); M. V. Arnim and R. Ahlrichs, J. Comp. Chem. **19**, 1746 (1998); F. Weigend, Phys. Chem. Chem. Phys. **4**, 4285 (2002).
- <sup>24</sup>N. Lorente and M. Persson, Phys. Rev. Lett. **85**, 2997 (2000).
- <sup>25</sup>H. Shimotani, T. Ito, Y. Iwasa, A. Taninaka, H. Shinohara, E. Nishibori, M. Takata, and M. Sakata, J. Am. Chem. Soc. **126**, 364 (2004).
- $^{26} \rm{The}$  calculated energy levels of  $C_{80}$  do not change significantly on adsorption (cf. Ref. [10]). Particularly, the HOMO and the lowest unoccupied molecular orbital (LUMO) of the free molecule are becoming the highest occupied and the lowest unoccupied orbitals of the adsorbed  $Ce_2@C_{80}$  (K. Muthukumar and J. A. Larsson, unpublished).
- <sup>27</sup>B. N. J. Persson, and A. Baratoff, Phys. Rev. Lett. **59**, 339 (1987).
- <sup>28</sup>M. Paulsson, T. Frederiksen, H. Ueba, N. Lorente, and M. Brandbyge, Phys. Rev. Lett. 100, 226604 (2008).
- <sup>29</sup>N. Okabayashi, Y. Konda, and T. Komeda, Phys. Rev. Lett. 100, 217801 (2008).
- <sup>30</sup>A. Gagliardi, G. C. Solomon, A. Pecchia, T. Frauenheim, A. Di Carlo, N. S. Hush, and J. R. Reimers, Phys. Rev. B 75, 174306 (2007).
- <sup>31</sup>E. Nishibori, M. Takata, M. Sakata, A. Taninaka, and H. Shinohara, Angew. Chem., Int. Ed. Engl. 40, 2998 (2001).